Asian Journal of Chemistry; Vol. 24, No. 2 (2012), 492-498

ASIAN JOURNAL OF CHEMISTRY

www.asianjournalofchemistry.co.in

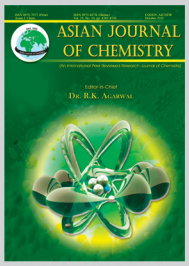

Reaction of Acetaldehyde with Palladium: A Density Functional Theoretical Study

GUO-LIANG DAI* and CHUAN-FENG WANG

School of Pharmaceutical and Chemical Engineering, Taizhou University, Linhai 317000, P.R. China

*Corresponding author: E-mail: daigl@tzc.edu.cn

(*Received*: 10 January 2011; *Accepted*: 3 October 2011) AJC-10467

The reaction mechanism of the palladium atom with acetaldehyde has been investigated with a DFT approach. All the stationary points are determined at the UB3LYP/ECP/6-311++G** level of the theory. Both ground and excited state potential energy surfaces are investigated in detail. The present results show that the reaction of acetaldehyde with palladium start with the formation of a η^2-CH_3CHO-metal complex, followed by C-C, aldehyde C-H, methyl C-H and C-O activation. These reactions can lead to four different products (PdCO + CH_4, $PdCOCH_3$ + H, $PdCHOCH_2$ + H, $PdCOCH_2$ + H_2). The present results may be helpful in understanding of the mechanism of the reaction of acetaldehyde with palladium and further experimental investigation of the reaction.

Key Words: DFT, Potential energy surfaces, Palladium, Acetaldehyde.

INTRODUCTION

Due to the great importance in catalytic and material science, the chemistry of interaction of gas-phase transition metal atoms and cations with hydrocarbon molecules has drawn great attention both in theoretical and experimental researches area[1-6]. For better understanding the fundamental aspects of this reaction, several studies have been reported on the investigation of the relevant mechanism[7-20]. As one of the simple carbonyl-containing organic molecules, acetaldehyde is used in many practical application fields such as organic synthesis, catalysis, *etc*. Since catalytic hydrogenation of carbon monoxide as well as C-H activation of aldehydes is usually promoted by metal-bearing catalysts, it is interesting and instructive to explore the reactions of gas-phase transition metal cations and atoms with aldehyde, which may lead to a better understanding of fundamental aspects of elementary transition metal reactions initiated by C-H insertion. Earlier studies[6-11] have focused mainly on the reactions between acetaldehyde and first row transition metal cations such as Co^+, Fe^+, Cr^+, Ti^+ and Ni^+. Some experimental techniques such as ion beam mass spectrometry and crossed-beam, have revealed that decarbonylation of acetaldehyde to yield $CH_4 + MCO^+$ is a dominant process at low energy condition[6]. Based on these experiments, Guo *et al.*[7-9] have theoretically investigated the gas-phase reaction of Co^+, Fe^+, Ti^+, Cr^+ and Ni^+ with acetaldehyde to reveal the corresponding mechanism. Their results show that for Co^+, Fe^+ and Cr^+, decarbonylation proceeds through C-C activation rather than aldehyde C-H activation, whereas both C-C and aldehyde C-H activation may result in the decarbonylation of acetaldehyde by Ni^+ cation. Compared with the first-row cation, heavier metal atoms and cations have received less attention and only a few theoretical and experimental studies have been reported[12-14]. Bayse *et al.*[14] have investigated the reaction between yttrium atom and acetaldehyde in detail. Their DFT calculations based on crossed molecular beams experiments predict the CO elimination to be the most exoergic channel, with the H_2 elimination products being slightly higher in energy. It should be noted that in their study, no CH_4 + YCO products channel was observed, which is quite different from the observations of reaction of the first row transition metal with acetaldehyde.

From the previous experimental and theoretical studies on the decarbonylation of acetaldehyde by first row cations and the larger transition-metal yttrium, it is clear that the transition metal change from first row to metal yttrium leads to the reaction change in mechanism both in early and late reaction stages. In addition, previous studies mainly focused on the reaction between first row cations and aldehyde, studies of the reaction between aldehyde and neutral are still scarce. Actually, the charge may often affect the mechanistic details. Therefore, it is necessary to extend the research to the reaction between neutral and aldehyde.

To the best of our knowledge, the previous investigation mainly focused on the first row elements, few studies with second row metals but yttrium have been performed in this reaction system. As is known, the metal yttrium can usually be categorized as a lanthanum analogous metal because of its similar chemical properties. Therefore, the research on typical

second-row metal and aldehyde reaction has important theoretical and experimental significances. Palladium is typical second-row late transition metal. Can a similar reaction mechanism be applicable to the reactions of Pd and Y atoms with acetaldehyde? What are the different behaviours between them? Prompted by these questions, we investigated the reactions of palladium atom with acetaldehyde by using DFT methods in detail in order to shed some light on these reactions. Although there is no experimental study reported on the reaction of palladium atom with acetaldehyde, a detail theoretical study on the reactions of palladium atom with acetaldehyde is interesting and important since palladium is a typical representative of the second-row late transition metal, the calculated results are expected to forecast further experimental findings and to give new suggestions that could not be reached experimentally under the considered conditions.

COMPUTATIONAL METHOD

The potential energy surface for the reaction has been considered in detail. All molecular geometries (reactants, intermediates, transition states and products) were optimized by employing the UB3LYP density functional theory method[21]. In all of our calculations, the 6-311++G** basis set was used for the hydrogen, carbon and oxygen atoms, the effective core potentials (ECP) of Stuttgart[22] basis set was used for the palladium, the 5*s* and 4*d* in palladium were treated explicitly by a (8*s*7*p*6*d*) Gaussian basis set contracted to [6*s*5*p*3*d*]. The previous calculations have shown that this basis set provides accurate results[23]. For all the species involved in the reaction, the enthalpies at 0 K is discussed in our study. The harmonic vibration analyses were performed at the same level of theory for all optimized stationary points to determine their properties (minimum or first-order saddle point) and to evaluate the zero-point vibrational energies (ZPEs). To verify whether the located transition states connected the expected minima, intrinsic reaction coordinate (IRC) calculations were carried out for each transition state at the same level[24]. All calculations in the present study were performed using the Gaussian 03 program[25].

RESULTS AND DISCUSSION

The optimized geometries of the stationary points over the potential energy surfaces (PESs) for the reaction of acetaldehyde with palladium are depicted in Fig. 1. The profiles of the potential energy surface are shown in Fig. 2. We also inspected the values of $<S^2>$ for all species involved in the reaction and found that the deviation of $<S^2>$ is less than 5 %. This shows that spin contamination is small in all the calculations.

As shown in Fig. 2, the present reaction starts with the formation of a η^2-CH_3CHO-metal encounter complex IM1. From Fig. 1(a) and Fig. 1(b), one can see that in ^{1}IM1 or ^{3}IM1, the palladium atom bonds with the carbon and oxygen simultaneously. As a result of oxygen polarizing charge toward palladium, the C-O bond is weakened and is lengthened by 0.033 Å and 0.101 Å in ^{1}IM1 and ^{3}IM1, respectively. Energetically, ^{1}IM1 lies 33.4 kcal/mol lower than the separate reactants of ^{1}Pd + CH_3CHO. For ^{1}IM1, it is computed to be 55.4 kcal/mol more stable than the corresponding triplet initial complex ^{3}IM1. It should be pointed out that although several trials were undertaken to search for possible transition states that connect reactants and IM1, no such transition states were obtained. Obviously, the formation of IM1 is a barrier-free exothermic reaction. Once the η^2-CH_3CHO-metal complex IM1 is formed, four possible reaction pathways can be followed by C-C, aldehyde C-H, methyl C-H and C-O activation, which will be discussed over singlet and triplet potential energy surfaces respectively in the following text.

First, we will discuss the singlet PES in detail. The first product generated from the reaction between Pd and CH_3CHO was P1. As shown in Fig. 2(a), this reaction channel starts with the formation of a η^2-CH_3CHO-metal complex IM1, along this reaction pathway, the Pd atom can insert into the C-C bond *via* a transition state $^1TS_{12}$. From Fig. 1(a), one can see the bond distance between two carbon atoms in $^1TS_{12}$ is varies from 1.504 to 2.124 Å. This indicates that the C-C bond is activated. The unique imaginary frequency is 313.2i cm^{-1} and the corresponding normal mode corresponds to the rupture of the C-C bond with the Pd atom inserting into it. For the inserted intermediate ^{1}IM2, the ground state is ^{1}A' with C_1 symmetry and it is 16.6 kcal/mol more stable in energy than the ground state reactants ^{1}Pd + CH_3CHO. As shown in Fig.1(a), the C-C distance in ^{1}IM2 is lengthened to 2.780 Å, which means that this bond has ruptured thoroughly. The two calculated Pd-C bonds are 1.968 and 1.908 Å, respectively, NBO analysis of this complex shows that the Pd interacts with these two atoms. Along this reaction coordinate, the C-C bond activation is followed by a H-shift to form ^{1}IM6, with an energy barrier of 21.9 kcal/mol. From Fig. 1(a), one can see that *via* the transition state $^1TS_{26}$, there is an aldehyde hydrogen migration on to the carbon centre. In ^{1}IM6, the Pd atom coordinates with CO and CH_4 group simultaneously and this species is 58.6 kcal/mol more stable than the ground reactants. From Fig. 2(a), it is observed that the ^{1}IM6 is the lowest point along the singlet PES of the present reaction. The calculation shows that ^{1}IM6 can decompose in a barrierless process to P1 (^{1}PdCO + CH_4) directly, requiring energy of 7.9 kcal/mol. In earlier theoretical studies on the gas-phase reactions of acetaldehyde with first-row transition metal cations (such as Cr^+, Fe^+, Co^+, Ni^+), Guo *et al.*[7-9] reported that the decarbonylation process leading to $M^+(CO) + CH_4$ is highly exothermic. Bayse *et al.*[14] have examined the reaction between yttrium atom and CH_3CHO, both experimentally and theoretically. They found the formation of products H_3CYH + CO is spontaneously in energy, but no $Y(CO) + CH_4$ species were observed and no feasible $Y(CO) + CH_4$ formation channel was determined in their studies. Though no relevant experimental researches on palladium with aldehyde are available, from the above discussion, it is found though most of the species along this decarbonylation channel are computed to be below the separated ground reactants (^{1}Pd + CH_3CHO), the rate determining step along this branch, *i.e.*, the carbonyl H shift *via* $^1TS_{26}$, is calculated to be 21.9 kcal/mol above the ground reactants. It is proposed that the decarbonylation product can not form spontaneously in the reaction of palladium atom with acetaldehyde. So, compared with the yttrium metal, the palladium atom can't decarbonylate from aldehyde effectively.

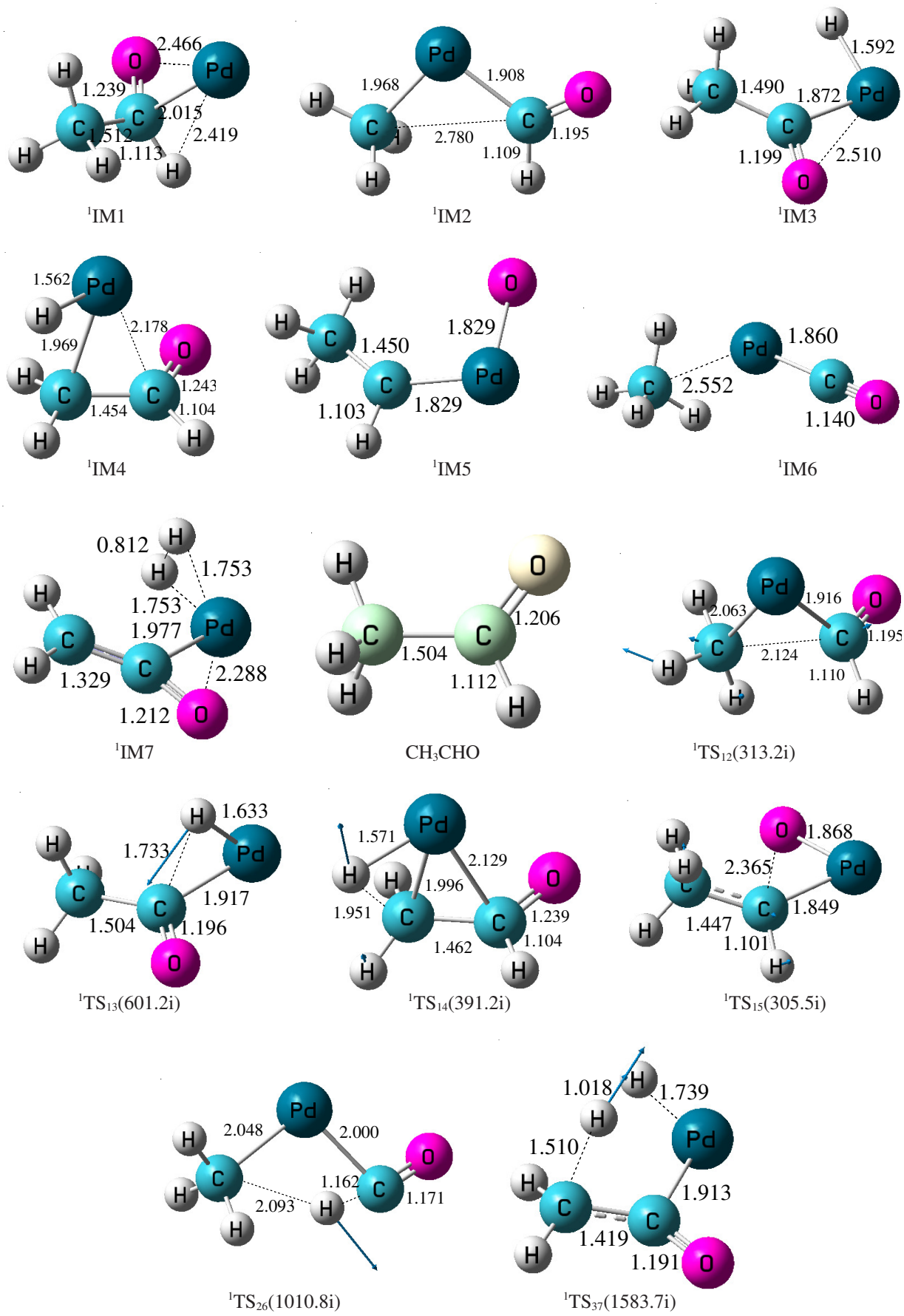

Fig. 1(a). Optimized geometries for the various stationary points located on the ^{1}Pd + CH_3CHO potential energy surfaces (distances in Å)

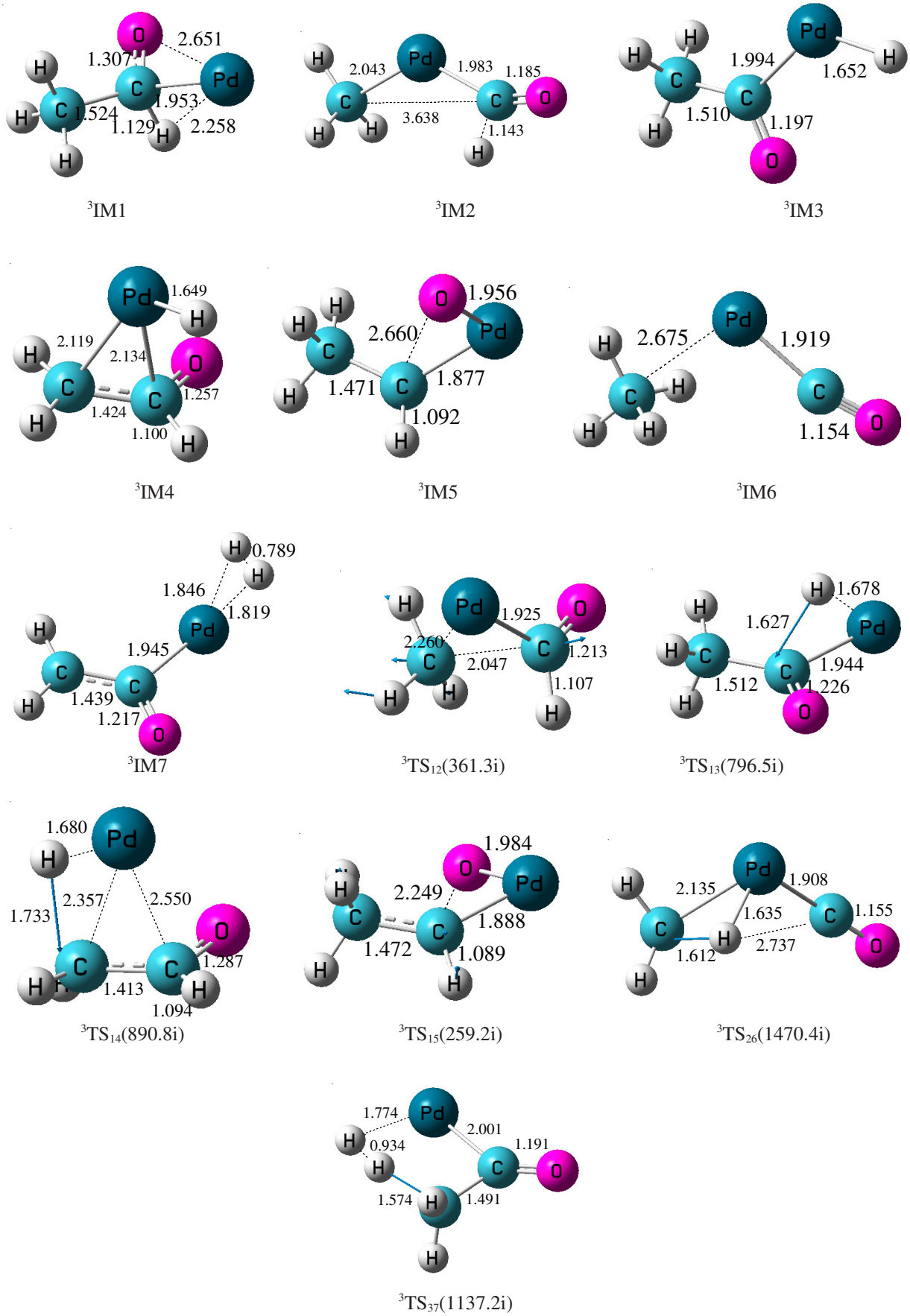

Fig. 1(b). Optimized geometries for the various stationary points located on the ^{3}Pd + CH_3CHO potential energy surfaces (distances in Å)

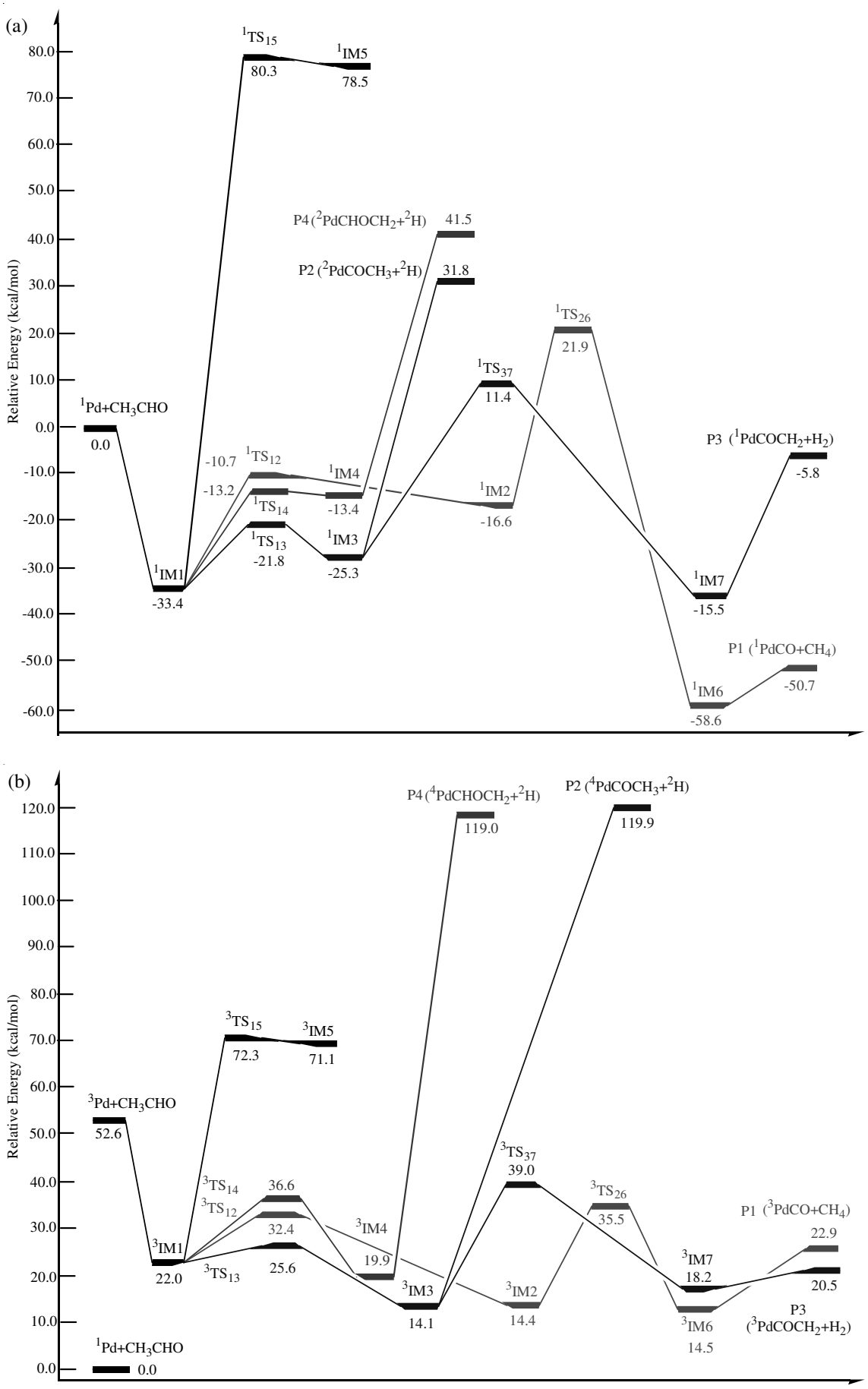

Fig. 2. Potential energy surface profiles for the reaction of (a) ^{1}Pd + CH_3CHO; (b) ^{3}Pd + CH_3CHO

TABLE-1
ENERGY OF VARIOUS COMPLEXES IN THE REACTION OF Pd ATOM WITH CH_3CHO (TOTAL ENERGY E_T, ZPE CORRECTIONS HAVE BEEN TAKEN INTO ACCOUNT, RELATIVE ENERGY E_R)

Species	E_T (Hartree)	E_R (kcal mol^{-1})
$^1Pd+CH_3CHO$	-279.9003669	0.0
$^1IM1$	-279.953553	-33.4
$^1IM2$	-279.926846	-16.6
$^1IM3$	-279.940676	-25.3
$^1IM4$	-279.921680	-13.4
$^1IM5$	-279.775315	78.5
$^1IM6$	-279.993747	-58.6
$^1IM7$	-279.925132	-15.5
$^1TS_{12}$	-279.917363	-10.7
$^1TS_{13}$	-279.935178	-21.8
$^1TS_{14}$	-279.921445	-13.2
$^1TS_{15}$	-279.772421	80.3
$^1TS_{26}$	-279.865461	21.9
$^1TS_{37}$	-279.882135	11.4
P1 ($^1PdCO+CH_4$)	-279.981204	-50.7
P2 ($^2PdCOCH_3+^2H$)	-279.849671	31.8
P3 ($^1PdCOCH_2+H_2$)	-279.909543	-5.8
P4 ($^2PdCHOCH_2+^2H$)	-279.834183	41.5
$^3Pd+CH_3CHO$	-279.8166201	52.6
$^3IM1$	-279.865322	22.0
$^3IM2$	-279.877496	14.4
$^3IM3$	-279.877826	14.1
$^3IM4$	-279.868602	19.9
$^3IM5$	-279.786991	71.1
$^3IM6$	-279.877289	14.5
$^3IM7$	-279.871363	18.2
$^3TS_{12}$	-279.848795	32.4
$^3TS_{13}$	-279.859623	25.6
$^3TS_{14}$	-279.841971	36.6
$^3TS_{15}$	-279.785217	72.3
$^3TS_{26}$	-279.843789	35.5
$^3TS_{37}$	-279.838244	39.0
P1 ($^3PdCO+CH_4$)	-279.863798	22.9
P2 ($^4PdCOCH_3+^2H$)	-279.709233	119.9
P3 ($^3PdCOCH_2+H_2$)	-279.867659	20.5
P4 ($^4PdCHOCH_2+^2H$)	-279.710722	119.0

With respect to the products P2($^1PdCOCH_2 + H_2$) and P3($^2PdCOCH_3 + ^2H$) formation channel, two possible channels have been confirmed, which originate from aldehyde C-H bond activation. In the former, the $^1IM1$ can interconvert to $^1IM3$ *via* $^1TS_{13}$, over a barrier height of 11.6 kcal/mol. In $^1IM3$, the Pd atom inserted into the aldehyde C-H bond with the relative energy of -25.3 kcal/mol. The next step corresponds to the isomerization between $^1IM3$ and $^1IM7$ *via* $^1TS_{37}$ directly, the relative energy of this transition state is 11.4 kcal/mol, which is 33.2 kcal/mol higher than that of the first step. Through this step, one methyl hydrogen atom is transfered toward the Pd atom and binds with the H atom that connects the metal centre, to form a H_2 molecule subsequently. From Fig. 2(a), one can see that the second step, *i.e.*, the process of $^1IM7$ formation is the rate determining step along this path. The species $^1IM7$ is 15.5 kcal/mol more stable than the ground reactants. The calculation shows that $^1IM7$ can decompose in a barrierless process to P2($^1PdCOCH_2 + H_2$) directly, requiring energy of 9.7 kcal/mol.

Another exit of $^3IM3$ is direct rupture of the H-$PdCOCH_3$ bond to generate product P3($^2PdCOCH_3 + ^2H$) and this dissociation process is computed to be endothermic by 57.1 kcal/mol. Compared with the P2 formation channel mentioned above, one can see this dissociation energy is higher than the methyl H-shift energy barriers (57.1 *vs.* 36.7 kcal/mol), Clearly, starting from the complex $^1IM3$, the reaction channel which lead to P3($^2PdCOCH_3 + 2H$) formation through the aldehyde C-H activation is more competitive.

We now turn to the methyl C-H activation channel, which may lead to product P4 formation. It is very clear from Fig. 2(a) that this route pass through metal-mediated methyl hydrogen migration followed by the non-reactive-dissociation. Initial complex $^1IM1$ and intermediate $^1IM4$ are connected through a direct, one-step methyl hydrogen shift occuring *via* saddle point $^1TS_{14}$. Geometrically, the activation C-H bond is elongated to 1.951 Å, synchronously, the distance between palladium and hydrogen atoms is shortened to 1.571 Å. The imaginary frequency of $^1TS_{14}$ is 391.21 cm^{-1} and the normal mode corresponds to the rupture of methyl C-H bond with the result of palladium binding with the hydrogen atom. One exit of $^1IM4$ is direct rupture of the H-Pd bond to account for the product P4 ($^2PdCHOCH_3 + 2H$), but this is a greatly endothermic process with the dissociation energy of 54.9 kcal/mol, so the formation of product P4 is rather difficult.

Previous studies of M (or M^+) + CH_3CHO mainly focused on the C-C or C-H activation reaction, which may lead to formation of $HMCH_3$ + CO or H + $MCOCH_3$. In the present study, it is also explored the possibility of aldehyde C-O bond activation mechanism. Originating from $^1IM1$, the C-O bond activation species, $^1IM5$, can be formed by the insertion of Pd atom into the aldehyde C-O bond. Energetically, the transition state ($^1TS_{15}$) is calculated to be 80.3 kcal/mol over the energies of the ground reactants. Obviously, in the reaction between Pd and CH_3CHO, the aldehyde C-O activation is not a feasible pathway. From other three routes which lead to formation of C-C and C-H activation intermediates, one can see that the Pd centre inserts into the aldehyde C-H *via* $^1TS_{13}$, is lower by 11.1 and 8.6 kcal/mol than that of the C-C ($^1TS_{12}$) and methyl C-H ($^1TS_{14}$) activation steps respectively. According to the exponential law of reaction rate [$k = Aexp(-E_a/RT)$], the reaction rate from $^1TS_{13}$ is approximately 1.4×10^8 and 1.9×10^6 times as fast as that from $^1TS_{12}$ and $^1TS_{14}$ at room temperature, respectively. Clearly, starting from the η^2-CH_3CHO-metal complex $^1IM1$, the channel which leads to $^1IM3$ formation through aldehyde C-H activation is more feasible than that of the C-C and methyl C-H activation. In addition, when compared the two channels which lead to products P1 and P3 formation, one can see that the rate-determing step energy barrier of the former is 10.5 kcal/mol higher than that of the later ($^1TS_{26}$ *vs.* $^1TS_{37}$), so we propose P3 should be the main product over the singlet potential energy surface.

Similar with that on the singlet PES, we also located possible activation channels on the triplet one. As shown in Fig. 1(b) and Fig. 2(b), the reaction mechanism on this PES is in general similar with that of the singlet one. The reaction starts with a η^2-CH_3CHO-metal complex followed by C-C, aldehyde C-H, methyl C-H and C-O activation. Comparing all the channels shown in Fig. 2(b), it is clear that the C-C insertion branch which leads to products P1($^3PdCO + CH_4$) is most feasible. Obviously, the Pd is more effective in

decarbonylation of acetaldehyde over triplet PES, this is quite different from that of the singlet one, over which dehydrogenation is dominating.

From Fig. 2(a) and 2(b), one can see most of the species (except TS_{15} and IM5) involved in the reaction on the singlet PES, lie below the analogues on the triplet one. Obviously, the singlet pathway is energetically preferred with respect to the corresponding triplet one. As the initial complex ^{1}IM1 is 22.0 kcal/mol lower than ^{3}IM1, while TS_{15} and IM5 in singlet are higher than triplet analogues 8.0 and 7.4 kcal/mol, respectively, we speculate that the intersystem singlet-triplet crossing occurs during the process of $^1IM1 \rightarrow {}^3TS_{15}$. However, from the above discussion, one can see the aldehyde C-O activation is most different due to the relative high rate determining barrier both on singlet and triplet PESs, so, this intersystem crossing is of no importance for the reaction mechanism.

Conclusion

In the present study, the reaction mechanisms between Pd atom and CH_3CHO have been investigated in detail, both on singlet and triplet PESs. The reaction of acetaldehyde with palladium is expected to proceed over the singlet PES. Originating from the intermediate complex ^{1}IM1, initial C-C bond insertion may lead to decarbonylation products $^1PdCO + CH_4$. Present calculations confirm three channels for C-H bond activation, among which the reaction occurs through Pd insertion into aldehyde C-H, followed by a methyl H-shift that yields P3($^1PdCOCH_2 + H_2$) is most feasible. Because of the high energy barrier compared with the C-C and C-H insertion reactions, the aldehyde C-O activation pathway may be neglectable. Obviously, the C-H activation pathway lead to formation of P3 ($^1PdCOCH_2 + H_2$) serves as a major channel because of the relative low energy barrier and dissociation energy. So, the most feasible channel should be described as: $^1Pd + CH_3CHO \rightarrow {}^1IM1 \rightarrow {}^1TS_{13} \rightarrow {}^1IM3 \rightarrow {}^1TS_{37} \rightarrow {}^1IM7 \rightarrow$ P3 ($^1PdCOCH_2 + H_2$).

ACKNOWLEDGEMENTS

This work was supported by the Zhejiang Provincial Natural Science Foundation of China under grant No. Y4090387 and No. Y4100508.

REFERENCES

1. Q. Zhang and M.T. Bowers, *J. Phys. Chem.*, **A108**, 9755 (2004).
2. L.F. Halle, W.E. Crowe, P.B. Armentrout and J.L. Beauchamp, *Organometallics*, **3**, 1694 (1984).
3. D.M. Sonnenfroh and J.M. Farrar, *J. Am. Chem. Soc.*, **108**, 3521 (1986).
4. M.R. Sievers, L.M. Jarvis and P.B. Armentrout, *J. Am. Chem. Soc.*, **120**, 4251 (1998).
5. C.L. Haynes, E.R. Fisher and P.B. Armentrout, *J. Am. Chem. Soc.*, **118**, 3269 (1996).
6. M.A. Tolbert and J.L. Beauchamp, *J. Phys. Chem.*, **90**, 5015 (1986).
7. L.M. Zhao, R.R. Zhang, W.Y. Guo, S.J. Wu and X.Q. Lu, *Chem. Phys. Lett.*, **414**, 28 (2005).
8. L.M. Zhao, W.Y. Guo, R.R. Zhang, S.J. Wu and X.Q. Lu, *Chem. Phys. Chem.*, **7**, 1345 (2006).
9. X.F. Chen, W.Y. Guo, L.M. Zhao, Q.T. Fu and Y. Ma, *J. Phys. Chem.*, **A111**, 3566 (2007).
10. Y. Ma, W.Y. Guo, L.M. Zhao, S.Q. Hu, J. Zhang, Q.T. Fu and X.F. Chen, *J. Phys. Chem.*, **A111**, 6208 (2007).
11. X.F. Chen, W.Y. Guo, T.F. Yang and X.Q. Lu, *J. Phys. Chem.*, **A112**, 5312 (2008).
12. C.A. Bayse, *J. Phys. Chem.*, **A106**, 4226 (2002).
13. J.J. Schroden, M. Teo and H.F. Davis, *J. Chem. Phys.*, **117**, 9258 (2002).
14. J.J. Schroden, H.F. Davis and C.A. Bayse, *J. Phys. Chem.*, **A111**, 11421 (2007).
15. M. Porembski and J.C. Weisshaar, *J. Phys. Chem.*, **A105**, 6655 (2001).
16. H.U. Stauffer, R.Z. Hinrichs, P.A. Willis and H.F. Davis, *J. Chem. Phys.*, **111**, 4101 (1999).
17. H.U. Stauffer, R.Z. Hinrichs, J.J. Schroden and H.F. Davis, *J. Phys. Chem.*, **A104**, 1107 (2000).
18. P.A. Willis, H.U. Stauffer, R.Z. Hinrichs and H.F. Davis, *J. Phys. Chem.*, **A103**, 3706 (1999).
19. R.Z. Hinrichs, J.J. Schroden and H.F. Davis, *J. Am. Chem. Soc.*, **125**, 861 (2003).
20. J.J. Schroden, M. Teo and H.F. Davis, *J. Phys. Chem.*, **A106**, 11695 (2002).
21. A.D. Becke, *J. Chem. Phys.*, **98**, 1372 (1993).
22. M. Dolg, H. Stoll, A. Savin and H. Preuss, *Theor. Chim. Acta*, **75**, 173 (1989).
23. G.L. Dai, H. Yan, A.G. Zhong and C.F. Wang, *Asian. J. Chem.*, **22**, 7187 (2010).
24. K. Fukui, *Acc. Chem. Res.*, **14**, 363 (1981).
25. M.J. Frisch, G.W. Trucks, H.B. Schlegel, G.E. Scuseria, M.A. Robb, J.R. Cheeseman, J.A. Montgomery, Jr., T. Vreven, K.N. Kudin, J.C. Burant, J.M. Millam, S.S. Iyengar, J. Tomasi, V. Barone, B. Mennucci, M. Cossi, G. Scalmani, N. Rega, G.A. Petersson, H. Nakatsuji, M. Hada, M. Ehara, K. Toyota, R. Fukuda, J. Hasegawa, M. Ishida, T. Nakajima, Y. Honda, O. Kitao, H. Nakai, M. Klene, X. Li, J.E. Knox, H.P. Hratchian, J.B. Cross, V. Bakken, C. Adamo, J. Jaramillo, R. Gomperts, R.E. Stratmann, O. Yazyev, A.J. Austin, R. Cammi, C. Pomelli, J.W. Ochterski, P.Y. Ayala, K. Morokuma, G.A. Voth, P. Salvador, J.J. Dannenberg, V.G. Zakrzewski, S. Dapprich, A.D. Daniels, M.C. Strain, O. Farkas, D.K. Malick, A.D. Rabuck, K. Raghavachari, J.B. Foresman, J.V. Ortiz, Q. Cui, A.G. Baboul, S. Clifford, J. Cioslowski, B.B. Stefanov, G. Liu, A. Liashenko, P. Piskorz, I. Komaromi, R.L. Martin, D.J. Fox, T. Keith, M.A. Al-Laham, C.Y. Peng, A. Nanayakkara, M. Challacombe, P.M.W. Gill, B. Johnson, W. Chen, M.W. Wong, C. Gonzalez and J.A. Pople, Gaussian 03, Revision B04, Gaussian Inc., Pittsburgh, PA (2003).